Ray and Wave Tomograms of a Deep Alpine Valley

BLEIBINHAUS, F.[1], HILBERG, S.[1] & STILLER, M.[2]

[1] Universität Salzburg, Fachbereich Geologie und Geographie, Hellbrunnerstr. 34, A-5020 Salzburg
[2] GeoForschungsZentrum Potsdam, Telegrafenberg, E 252, D-14473 Potsdam

Introduction

In late 2009 we conducted a refraction-and-reflection-seismic survey in the Salzach Valley in the Eastern Alps near Zell am See. The goal was to image structure and depth of the sedimentary infill, which we assumed to be ~ 300 m thick based on a comparison of the valley's proportions to other glacially deepened valleys from the region. This paper presents firsts inverse models from the refraction and wide-angle reflection data based on ray theory and full-waveform inversion. Results from reflection imaging and surface wave inversion will be discussed in a different paper.

Data acquisition and quality

The survey consists of a 3 km long stationary receiver line perpendicular to the valley's axis (Fig. 1). The close proximity of the profile to the N-S-trending part of the Zeller Basin is a result of logistic considerations. We assume nevertheless that the structural variations perpendicular to the profile are small and can be neglected. The line consists of two pieces of 216 and 48 channels, respectively, which are separated by railway tracks and a highway close to the Northern edge of the valley. Geophone spacing is 10 m, except for a 350 m wide gap near the railway, which was closed by a dozen continuously recording one-component stations manufactured by the GeoForschungsZentrum. We used 10 Hz and 14 Hz single

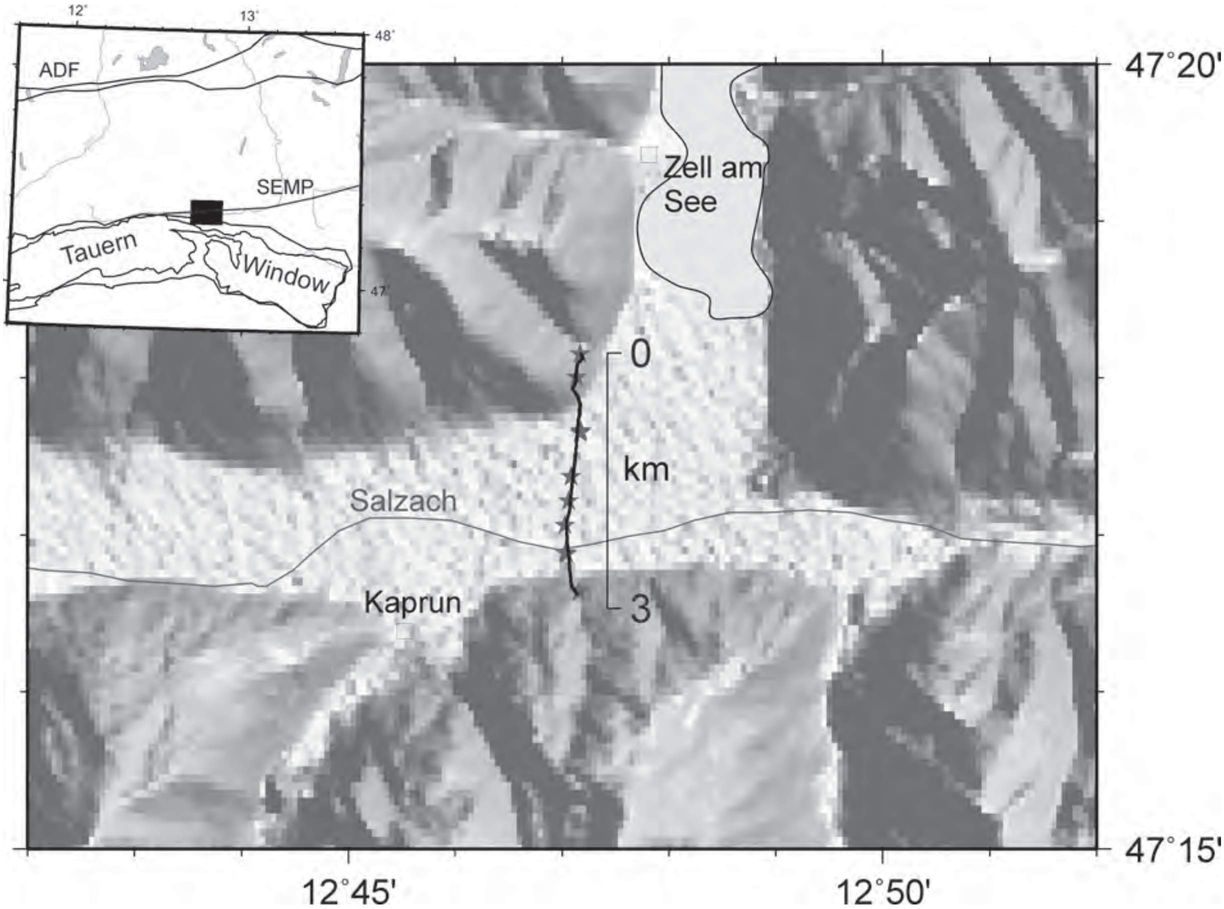

Fig. 1: Map of the survey area. Black line is receivers, stars are shot points.

geophones with the cable, and 4.5 Hz single geophones with the one-component stations. Eight refraction shots of 0.8-3.1 kg were observed with the full spread. For the reflection survey we used accelerated drop-weight sources, and we interspersed additional channels near the shot point to attain 5 m receiver-spacing in order to avoid aliasing of surface waves.

The refraction data is generally of high quality with good S/N in the 4-80 Hz frequency band. Fig. 2 displays two exemplary shots. The shots in the valley show a strong reflection from the bedrock. The refraction from the bedrock (Pg) is visible on all shots, though sometimes weak and difficult to detect. The direct wave in the sediments (Psed) exhibits a shadow zone in the Southern part of the valley (e.g., SP 4 at ~ 0.3 s near channel 170) indicative of a low-velocity-layer.

Ray Tomography

A total of 1500 first-arrival travel-times were extracted from the data to be used for diving-ray tomography. For the forward modelling we use an eikonal solver of Hole (1992). We choose the L2-norm of the traveltime misfit as objective function, and we use a damped LSQR matrix inversion to constrain an under-parameterized model, following the approach of Thurber (1983), with adaptations for irregular model parameterization by Bleibinhaus & Gebrande (2006). Our starting model is 1D with minor variations due to the irregular parameterization, the computation is 3D discontinuous model describes the valley much better than a smooth model.

In this refraction-and-reflection ray model, the maximum thickness of the sedimentary infill is 450 m. From the analysis of the reflector geometry in a series of inversions with different velocity and reflector node distributions we

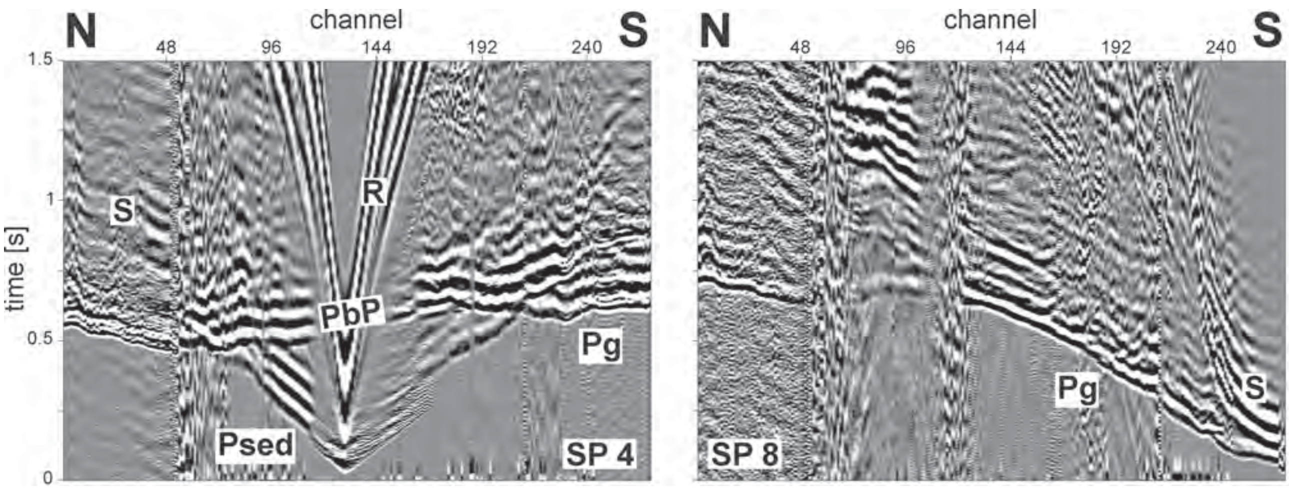

Fig. 2: Shot point 4 at the center of the valley (left) and shot point 8 at the Southern end of the line. Psed - direct P-wave through the sediments, Pg - refraction from the bedrock. PbP - reflection from the bedrock, partially superposed by R - Rayleigh waves. The stations on bedrock often observe S-waves. Note that there is a gap in the line near the railway/highway (~ chan 50) where the station distribution is sparse and irregular. The total spread is 2.8 km.

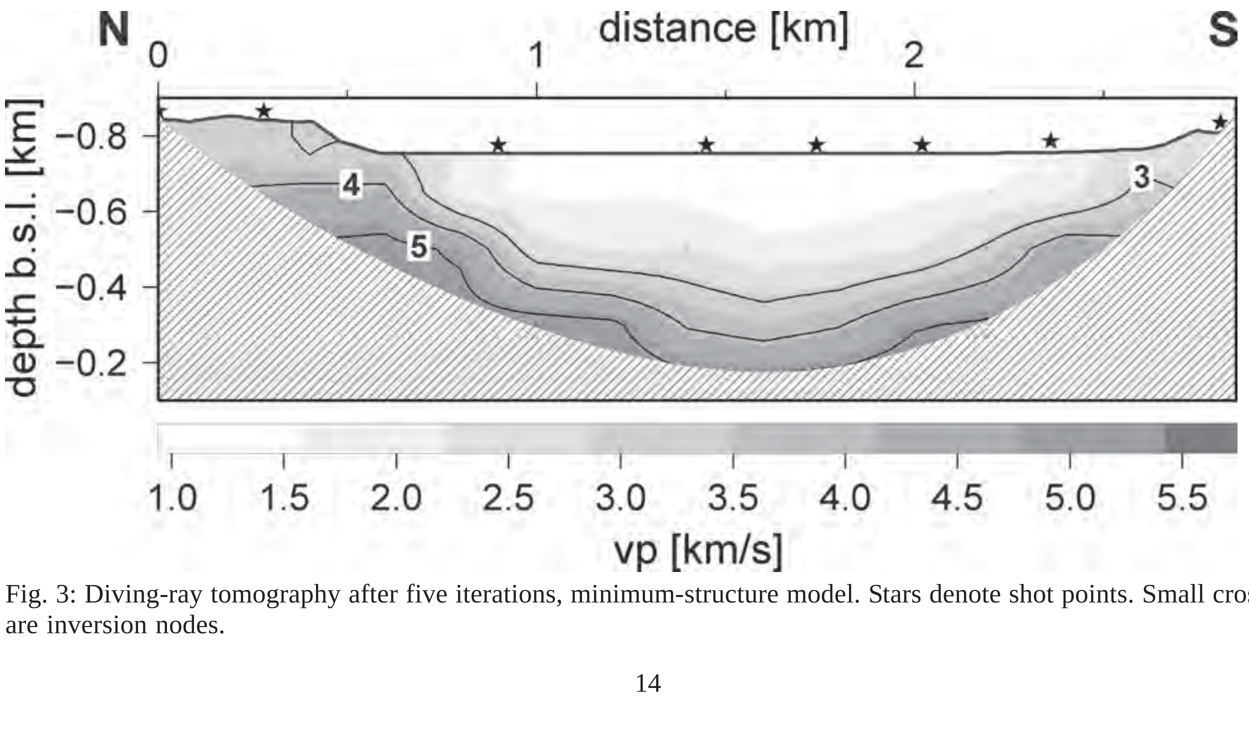

Fig. 3: Diving-ray tomography after five iterations, minimum-structure model. Stars denote shot points. Small crosses are inversion nodes.

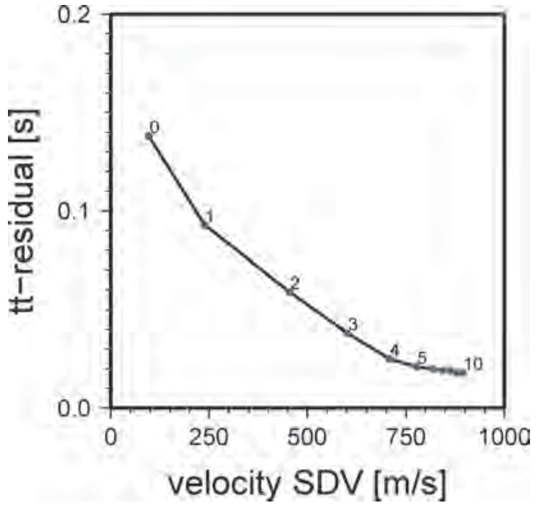

Fig. 4: Traveltime residual versus model heterogeneity (average velocity standard deviation at different depth levels) for different inversion iterations. After five iterations the reduction of the traveltime residual becomes insignificant compared to the increase in model heterogeneity.

conclude that the uncertainty of the maximum thickness amounts to ~ 25 m. This is consistent with the results from the diving ray tomography, but much more accurate.

Waveform Tomography

The problem with reflector tomography is that the extraction of reflection travel times is a process that discards ambiguous data, and that the concept of a reflector imposes a certain amount of smoothness, whether real or not. While the good data fit in combination with the small number of model parameters strongly supports this approach, it is also clear that the fine scale structure is lost, including potential steps in the reflector topography. On top of that, the resolution assessment cannot account for the incompleteness that comes with travel time extraction, because it is always based on these travel times. Waveform tomography offers a way to account for all seismograms, and to recover the fine-scale structure of the earth, by modelling the full waveforms. We consider our data as very well suited for waveform inversion due to the broad bandwidth. At 4 Hz we propagate at most eight wavelengths through the model. This enables the inversion to also fix long-wavelength misfits that are part of the starting model, which we derive by diving-ray tomography. We use the L2-norm of the frequency-domain amplitudes as objective function, and we employ a 2D acoustic approach developed by Pratt (1996) that has been successfully applied to real long-offset data. However, we normalize the amplitudes before forming the objective function, such that we really invert for the phase as a function of frequency, a concept applied by Bleibinhaus et al. (2007) to suppress the problem with true amplitude processing of data with strong near-surface variability. In order to prepare the data for waveform inversion, we remove all shear-waves that we can identify, and we window the data around the first-arrivals, such that the inversion focuses on the P-wave and its early coda. The window length varies from 0.4 to 1 s, and it includes the reflection from the bedrock where it is not superposed by ground roll. The starting model from ray tomography and the final model after sequential inversion of 50 frequency components in the 4-28 Hz range are displayed in Fig. 6. The close proximity of the 3, 4, and 5 km/s contour lines in the waveform model indicates that the waveform inversion model converges towards a discontinuity. In contrast to the diving-ray tomography, the waveform model shows high P-wave velocities, and a steep gradient, also close to the surface, where the bedrock is exposed, particularly at the Northern shoulder. Neither the diving-ray tomography, nor the reflection tomography was able to reconstruct this shoulder, and it had to be included as a-priori information in the reflection tomography. Its reconstruction provides additional confidence in the

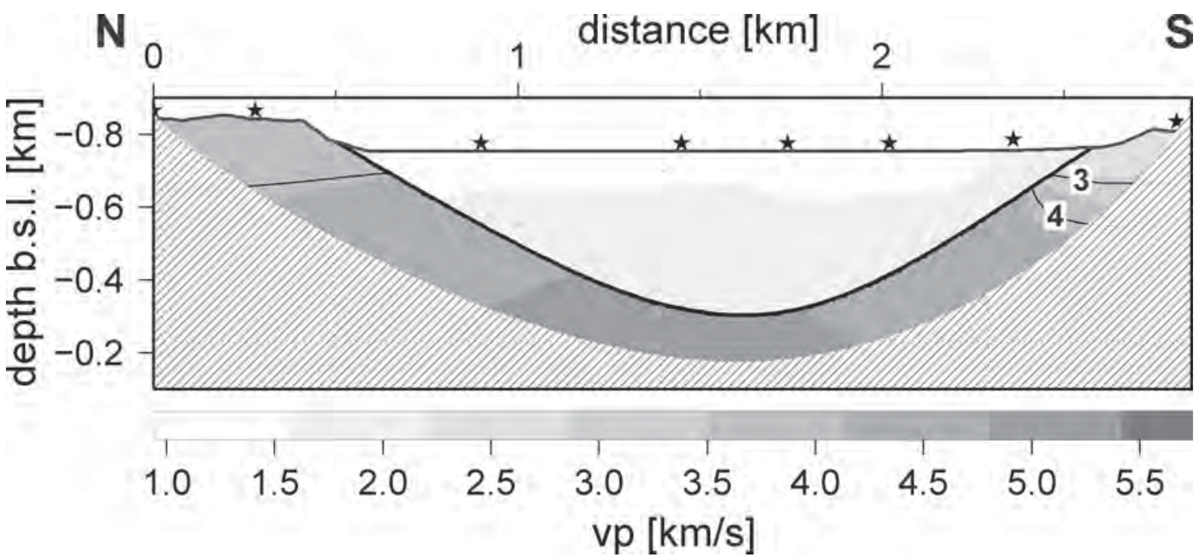

Fig. 5: Simultaneous reflection and refraction ray tomography after five iterations, minimum-structure model.

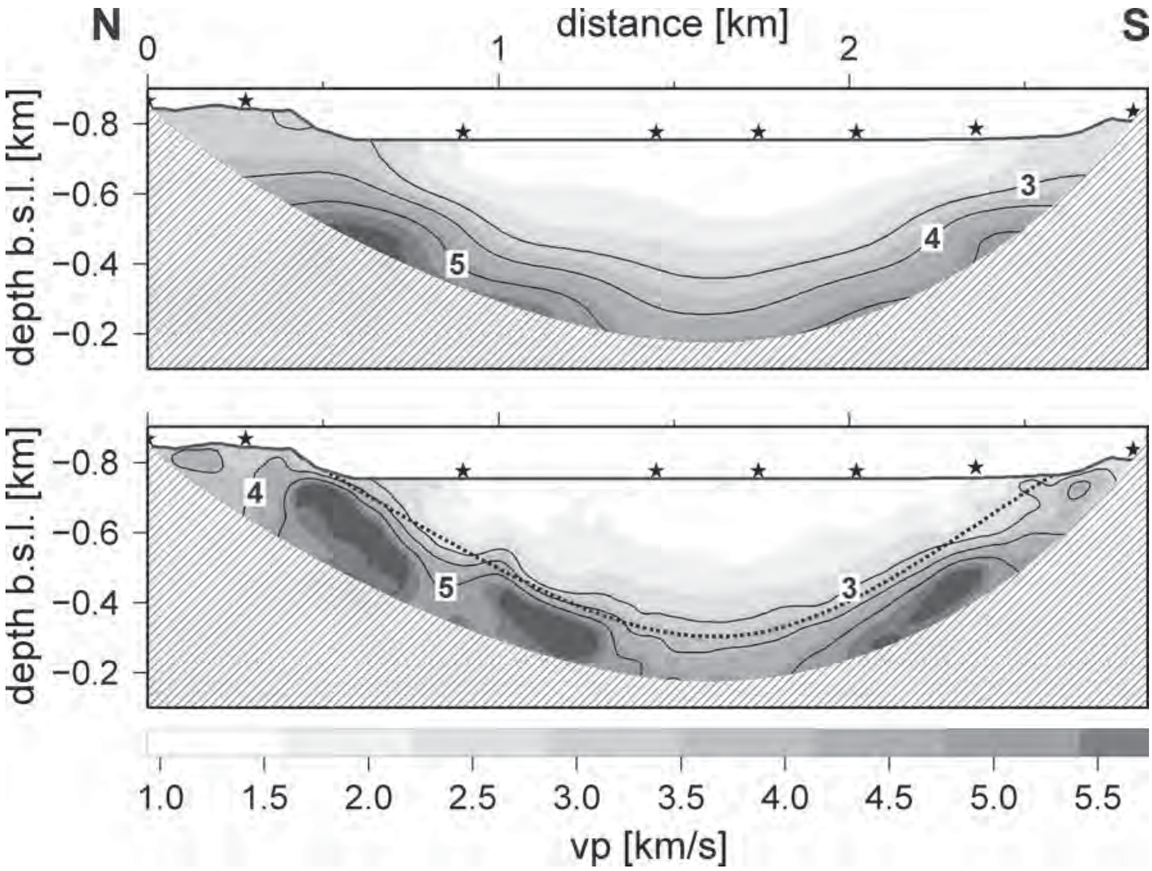

Fig. 6: Waveform inversion starting model (top) and final model (bottom). For comparison, a dashed line denotes the reflector position from ray tomography.

waveform model, which, otherwise, is largely consistent with the reflection tomography result, but provides much more detail, like the undulation of the top bedrock at 0.8 - 1 km distance. However, it is beyond the scope of this paper, to discuss those details. The most important features of the waveform model are the high-velocity zones, which indicate the bedrock. Their position and dip suggests that the reflector from ray tomography does not overestimate the sedimentary thickness.

Conclusions

The different tomography methods are largely consistent, but they provide a very different amount of detail and accuracy. Despite few and sparse shot points, waveform inversion produces reliable results due to the broad bandwidth of the signal, in particular the low frequencies. The models show that the maximum thickness of the postglacial sedimentary infill is about 450 m, which is 50% thicker than was expected.

Acknowledgements

We want to thank the field crews from Potsdam (Mike Hönig) and Salzburg (Bianca Heberer, Georg Gruber, Johannes Mayer, Hans Pum) for their tireless efforts. The high data quality would not have been possible without the professional drilling and shooting by Georg Zagler. We are grateful to GWU GmbH and Geoconsult ZT GmbH for lending off-road vehicles, and to Geocentricom and Pöyry Infra GmbH, for providing the shooting equipment.

References

Bleibinhaus, F. & Gebrande, H. (2006): Crustal structure of the Eastern Alps along the TRANSALP profile from wide-angle seismic tomography. - Tectonophysics, **414**: 51-69.

Bleibinhaus, F., Hole, J.A., Ryberg, T. & Fuis, G. (2007): Structure of the California Coast Ranges and San Andreas Fault at SAFOD from Seismic Waveform Inversion and Reflection Imaging. - J. Geophys. Res., **112**: B06315, doi:10.1029/2006JB004611.

Hole, J.A. (1992): Nonlinear High-Resolution 3-Dimensional Seismic Travel Time Tomography. - J. Geophys. Res., **97**(B5): 6553-6562.

Pratt, R.G., Song, Z.M., Williamson, P. & Warner, M. (1996): Two-dimensional velocity models from wide-angle seismic data by wavefield inversion. - Geophys. J. Int., **124**(2), 323-340.

Thurber, C.H. (1983): Earthquake Locations and 3-Dimensional Crustal Structure in the Coyote Lake Area, Central California. - J. Geophys. Res., **88**(B10): 8226-8236.